

## BRIEF REPORT

## A Dystroglycan Mutation Associated with Limb-Girdle Muscular Dystrophy

Yuji Hara, Ph.D., Burcu Balci-Hayta, Ph.D., Takako Yoshida-Moriguchi, Ph.D., Motoi Kanagawa, Ph.D., Daniel Beltrán-Valero de Bernabé, Ph.D., Hülya Gündeşli, M.S., Tobias Willer, Ph.D., Jakob S. Satz, Ph.D., Robert W. Crawford, B.S., Steven J. Burden, Ph.D., Stefan Kunz, Ph.D., Michael B.A. Oldstone, M.D., Ph.D., Alessio Accardi, Ph.D., Beril Talim, M.D., Francesco Muntoni, M.D., Haluk Topaloğlu, M.D., Pervin Dinger, Ph.D., and Kevin P. Campbell, Ph.D.

## SUMMARY

Dystroglycan, which serves as a major extracellular matrix receptor in muscle and the central nervous system, requires extensive O-glycosylation to function. We identified a dystroglycan missense mutation (Thr192→Met) in a woman with limb-girdle muscular dystrophy and cognitive impairment. A mouse model harboring this mutation recapitulates the immunohistochemical and neuromuscular abnormalities observed in the patient. In vitro and in vivo studies showed that the mutation impairs the receptor function of dystroglycan in skeletal muscle and brain by inhibiting the post-translational modification, mediated by the glycosyltransferase LARGE, of the phosphorylated O-mannosyl glycans on  $\alpha$ -dystroglycan that is required for high-affinity binding to laminin.

MUSCULAR DYSTROPHIES ARE GENETIC DISEASES CHARACTERIZED BY weakness and progressive degeneration of skeletal muscle. The transmembrane protein dystroglycan, which is ultimately cleaved into an  $\alpha$  and a  $\beta$  component, is a key link between the cytoskeleton and extracellular-matrix proteins that bear laminin globular domains (e.g., laminin, agrin, and neurexin).<sup>1,2</sup> The mucin domain of  $\alpha$ -dystroglycan is modified with numerous O-linked oligosaccharides that are essential for its normal function as an extracellular-matrix receptor in various tissues, including skeletal muscle and brain.<sup>2,3</sup> Hypoglycosylation of  $\alpha$ -dystroglycan and a consequent reduction of  $\alpha$ -dystroglycan binding to extracellular-matrix proteins are observed in patients with the Walker–Warburg syndrome, muscle–eye–brain disease, Fukuyama-type congenital muscular dystrophy, congenital muscular dystrophy types 1C and 1D, and limb-girdle muscular dystrophy 2I.<sup>2</sup> To date, genes encoding six putative and known glycosyltransferases (*POMT1*, *POMT2*, *POMGnT1*, *LARGE*, *FKTN*, and *FKRP*) have been shown to be responsible for approximately 50% of cases of these diseases, which are collectively referred to as secondary dystroglycanopathies<sup>4–11</sup> and which often feature brain abnormalities as well as muscular dystrophy. Despite recent advances in our understanding of the molecular mechanisms underlying secondary dystroglycanopathies, it remains unclear whether dystroglycan is the only target of these enzymes or whether other substrates contribute to the pathogenesis of these diseases.

Dystroglycan is known to be modified with several classes of oligosaccharides: N-glycans, mucin-type O-glycans, and O-mannosyl glycans.<sup>2</sup> The O-mannosyl gly-

From the Departments of Molecular Physiology and Biophysics (Y.H., T.Y.-M., M.K., D.B.-V.B., T.W., J.S.S., R.W.C., A.A., K.P.C.), Neurology (K.P.C.), and Internal Medicine (K.P.C.), and the Howard Hughes Medical Institute (K.P.C.), University of Iowa Roy J. and Lucille A. Carver College of Medicine, Iowa City; the Departments of Medical Biology (B.B.-H., H.G., P.D.), Pediatric Pathology (B.T.), and Pediatric Neurology (H.T.), Faculty of Medicine, Hacettepe University, Sıhhiye, Ankara, Turkey; the Molecular Neurobiology Program, Helen L. and Martin S. Kimmel Center for Biology and Medicine at the Skirball Institute of Biomolecular Medicine, New York University Medical School, New York (S.J.B.); the Institute of Microbiology, University Hospital Center and University of Lausanne, Lausanne, Switzerland (S.K.); the Department of Immunology and Microbial Science, Scripps Research Institute, La Jolla, CA (M.B.A.O.); and the Dubowitz Neuromuscular Centre, University College London Institute of Child Health, London (F.M.). Address reprint requests to Dr. Campbell at the University of Iowa Roy J. and Lucille A. Carver College of Medicine, 285 Newton Rd., 4283 CBRB, Iowa City, IA 52242, or at kevin-campbell@uiowa.edu.

Drs. Hara and Balci-Hayta contributed equally to this article.

N Engl J Med 2011;364:939-46.  
Copyright © 2011 Massachusetts Medical Society.

cans are thought to be responsible for dystroglycan's ligand-binding activity because the POMT1–POMT2 protein complex catalyzes the transfer of mannose to serine or threonine residues by means of an O-linkage.<sup>2</sup> We recently reported that maturation of  $\alpha$ -dystroglycan to its laminin-binding form requires a novel biosynthetic pathway involving phosphorylation on O-mannosyl glycans and that LARGE is crucial for further modification of phosphorylated O-mannosyl glycans on  $\alpha$ -dystroglycan.<sup>12</sup>

Here we report a missense mutation in the dystroglycan-encoding gene, *DAG1*, in a patient with limb-girdle muscular dystrophy and cognitive impairment. Our studies revealed that this substitution interferes with LARGE-dependent maturation of phosphorylated O-mannosyl glycans on  $\alpha$ -dystroglycan and leads to the disease-causing defect of  $\alpha$ -dystroglycan binding to laminin.

## METHODS

### CLINICAL INFORMATION

The patient initially received a diagnosis of limb-girdle muscular dystrophy with mental retardation.<sup>13</sup> Clinical data regarding this patient have been reported elsewhere.<sup>14</sup> (See also the Supplementary Appendix, available with the full text of this article at NEJM.org.) This study was approved by the institutional review board at Hacettepe University, and written informed consent was obtained from the patient's guardians.

### BIOCHEMICAL ANALYSIS

Biochemical analyses, including Western blotting, laminin-binding assays, and protein pull-down assays, were carried out as previously described.<sup>3,15</sup> (For details about the cell-culture and biochemical methods used, see the Supplementary Appendix.)

### MOUSE MODEL

Protocols for generating a knock-in mouse model harboring a mutation equivalent to that in our patient, as well as animal care and animal procedures, were approved by the University of Iowa Animal Care and Use Committee (see the Supplementary Appendix).

## RESULTS

We studied a Turkish patient with a relatively mild form of muscular dystrophy accompanied by cog-

nitive impairment (see Case 2 in Dinçer et al.<sup>14</sup>). Although immunofluorescence analysis showed that  $\alpha$ -dystroglycan was hypoglycosylated in this patient, no mutation was found in genes previously implicated in the pathogenesis of secondary dystroglycanopathies.<sup>14</sup> Since the dystroglycan-encoding gene, *DAG1*, is a plausible candidate gene, we investigated whether our patient harbored a causative mutation therein. Sequencing of the coding and noncoding regions of *DAG1* revealed a homozygous C-to-T missense mutation at position c.575, causing substitution of a methionine for a threonine at amino acid residue 192 (T192→M) of the protein (Fig. 1A). Both parents were heterozygous carriers of this mutated allele, and allele segregation in the family was consistent with recessive disease inheritance (Fig. 1B). The mutated threonine residue is located in the  $\alpha$ -dystroglycan N-terminal and is highly conserved across species (Fig. 1C).

We first assessed the effect of the newly identified  $\alpha$ -dystroglycan mutation in vitro, with respect to expression, post-translational processing, or both. To this end, we transiently expressed the full-length wild-type and T192→M dystroglycan proteins in dystroglycan-null myoblasts. Western blotting with an antibody that recognizes functionally glycosylated  $\alpha$ -dystroglycan (IIH6)<sup>3,15</sup> revealed considerably lower immunoreactivity for T192→M than for wild-type dystroglycan when similar amounts of protein were expressed (Fig. 1D). Biotinylation analysis revealed that the cell-surface expression of T192→M and wild-type dystroglycan was similar (Fig. 1A in the Supplementary Appendix). Thus, in myoblasts, the T192→M substitution affects neither protein localization nor protein stability, but it does impair post-translational modification. A laminin-binding assay confirmed that the T192→M mutation considerably reduces the effectiveness of dystroglycan as a laminin receptor (Fig. 1D, and Fig. 1B and 1C in the Supplementary Appendix).

We next assessed the effect of the T192→M mutation on functional modification of  $\alpha$ -dystroglycan in vivo by introducing a T190→M mutation (which corresponds to the human T192→M mutation) into the mouse *Dag1* gene (Fig. 2 in the Supplementary Appendix). Histologic analysis revealed hallmarks of muscular dystrophy, such as centrally nucleated fibers, in the mutant mice (Fig. 2A, and Fig. 3A and 4 in the Supplementary Appendix). Immunofluorescence and biochemical analyses showed that the mutated

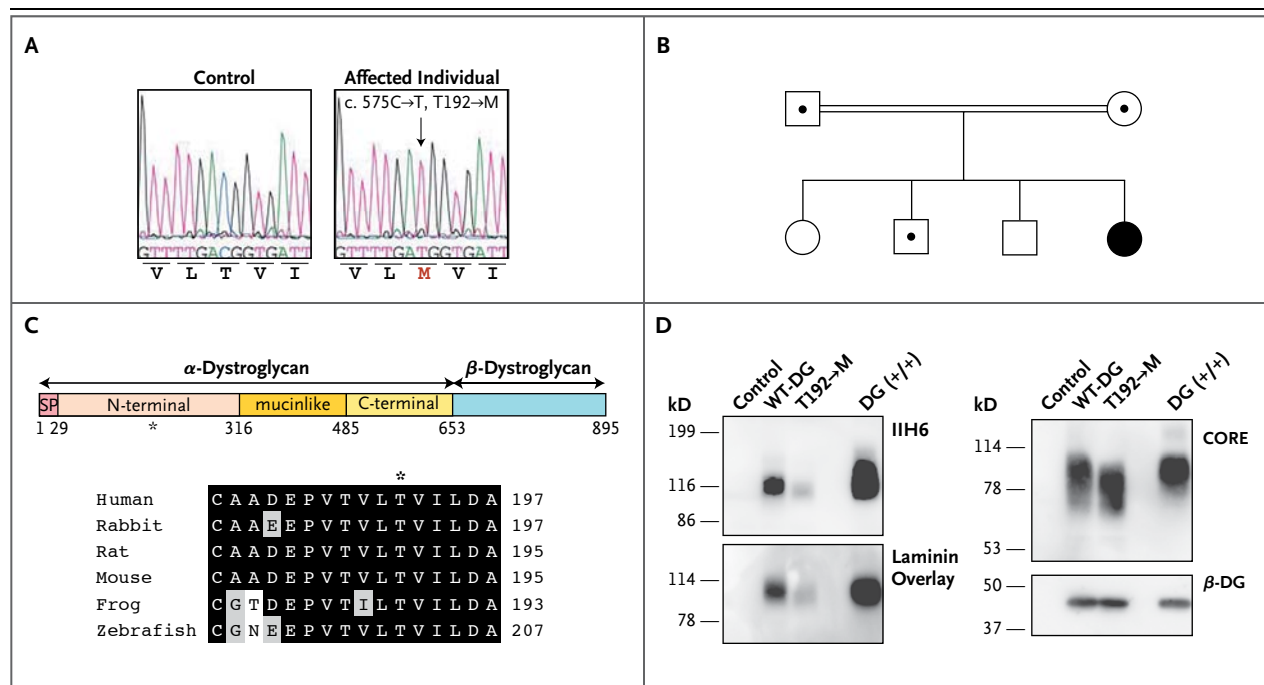


**Figure 1. Identification of a DAG1 Missense Mutation in a Woman with Limb-Girdle Muscular Dystrophy, and In Vitro Biochemical Characterization of the Encoded Protein.**

In Panel A, electrochromatograms reveal sequence variation in *DAG1*. A homozygous mutation, c.575C→T (arrow), leads to an amino acid change, T192→M. The T192→M variant was not detected in any of the 100 Turkish control subjects tested (200 chromosomes). Panel B shows the family pedigree. Squares denote male family members, and circles female family members; the double line indicates a consanguineous marriage; the black circle denotes the affected woman, and dots indicate heterozygous carriers. Panel C shows a schematic representation of a dystroglycan mutant protein (top). Human α-dystroglycan is composed of a signal peptide (SP) (amino acids 1 through 29), an N-terminal domain (amino acids 30 through 316), a mucinlike domain (amino acids 317 through 485), and a C-terminal domain (amino acids 486 through 653). The position of the patient's mutation (T192→M) is indicated by an asterisk. Amino acid residues are aligned flanking the codon affected by the T192→M missense mutation (bottom). Among these residues, black boxes denote identity and gray boxes similarity. Panel D shows a biochemical analysis of wild-type (WT-DG) and T192→M dystroglycan in dystroglycan-null myoblast cells. Functional modification of α-dystroglycan was evaluated by Western blotting with an antibody (IIH6) that recognizes only the glycosylated form of α-dystroglycan and by laminin-overlay assay. Overall expression of wild-type dystroglycan and T192→M dystroglycan was detected with the use of antibodies against the α-dystroglycan protein core (CORE) and antibodies against β-dystroglycan (β-DG).

α-dystroglycan was expressed at the skeletal-muscle sarcolemma but that both ligand-binding activity and IIH6 reactivity at this location were considerably decreased (Fig. 2B, and Fig. 3B and 5 in the Supplementary Appendix). Analysis of the uptake in the diaphragm of the membrane-impermeable Evans blue dye revealed disruption of the skeletal-muscle sarcolemma in the T190→M mice after exercise (Fig. 2C). The mutant mice also had marked impairment of exercise performance (e.g., reduced forelimb grip strength) (Fig. 2D). Mice heterozygous for the T190→M mutation did not have obvious muscle defects at the histologic level, despite a slight reduction in functional glycosylation of α-dystroglycan (Fig. 4 and 6 in the Supplementary Appendix). Thus, the T190→M muta-

tion caused skeletal-muscle abnormalities in mice that were consistent with those observed in our patient.

In addition to its role in skeletal muscle, dystroglycan is crucial for maintaining the structure and function of the brain and neuromuscular junctions.<sup>3,16-18</sup> Western blot and laminin-overlay analyses revealed that laminin-binding activity was significantly diminished in the brains of mice with the T190→M mutation (Fig. 3A). Morphologic analysis of the neuromuscular junctions revealed that the T190→M mutation interfered with their maturation; on staining of diaphragm samples with α-Bungarotoxin conjugated with Alexa Fluor 488 (Invitrogen), which tightly binds acetylcholine receptors, the neuromuscular junctions

in wild-type animals formed the expected pretzel-like structure, whereas those in the T190→M mice were round and immature (Fig. 3B and 3C, and Fig. 7 in the Supplementary Appendix). Consistent with impaired neuromuscular-junction maturation was the observation that the mutant mice had marked deficiencies in assays of neuromuscular function — for example, a reduction in retention time on a rotating-rod device (Fig. 3D). Furthermore, although no structural abnormality was evident in the brains of the T190→M mice (an observation that was consistent with the results on magnetic resonance imaging [MRI] of the patient's brain), these mice had abnormal hind-limb clasping, a phenotype common to mouse models featuring neurologic impairment (Fig. 8 in the Supplementary Appendix). Collectively, these results provide strong evidence that the mutation in the patient caused neurologic impairment as well as muscular dystrophy as a consequence of impaired  $\alpha$ -dystroglycan post-translational modification.

Dystroglycan is also expressed in cardiac muscle, where its function as an extracellular-matrix receptor is important for limiting activity-induced myocardial damage.<sup>19</sup> Given that some patients with mutations in *FKTN* and *FKRP* have dilated cardiomyopathy,<sup>20,21</sup> we analyzed cardiac tissue from T190→M mice. We observed no obvious signs of any pathological abnormality, such as fibrosis or uptake of Evans blue dye after exercise (Fig. 9 in the Supplementary Appendix). Moreover, in contrast to the observed effects in brain and skeletal muscle, laminin-binding activity was affected only minimally in the hearts of T190→M mice (Fig. 3A). Thus, it appears that normal cardiac function is maintained in T190→M knock-in mice and that the effects of the mutation on functional modification of  $\alpha$ -dystroglycan are tissue-dependent.

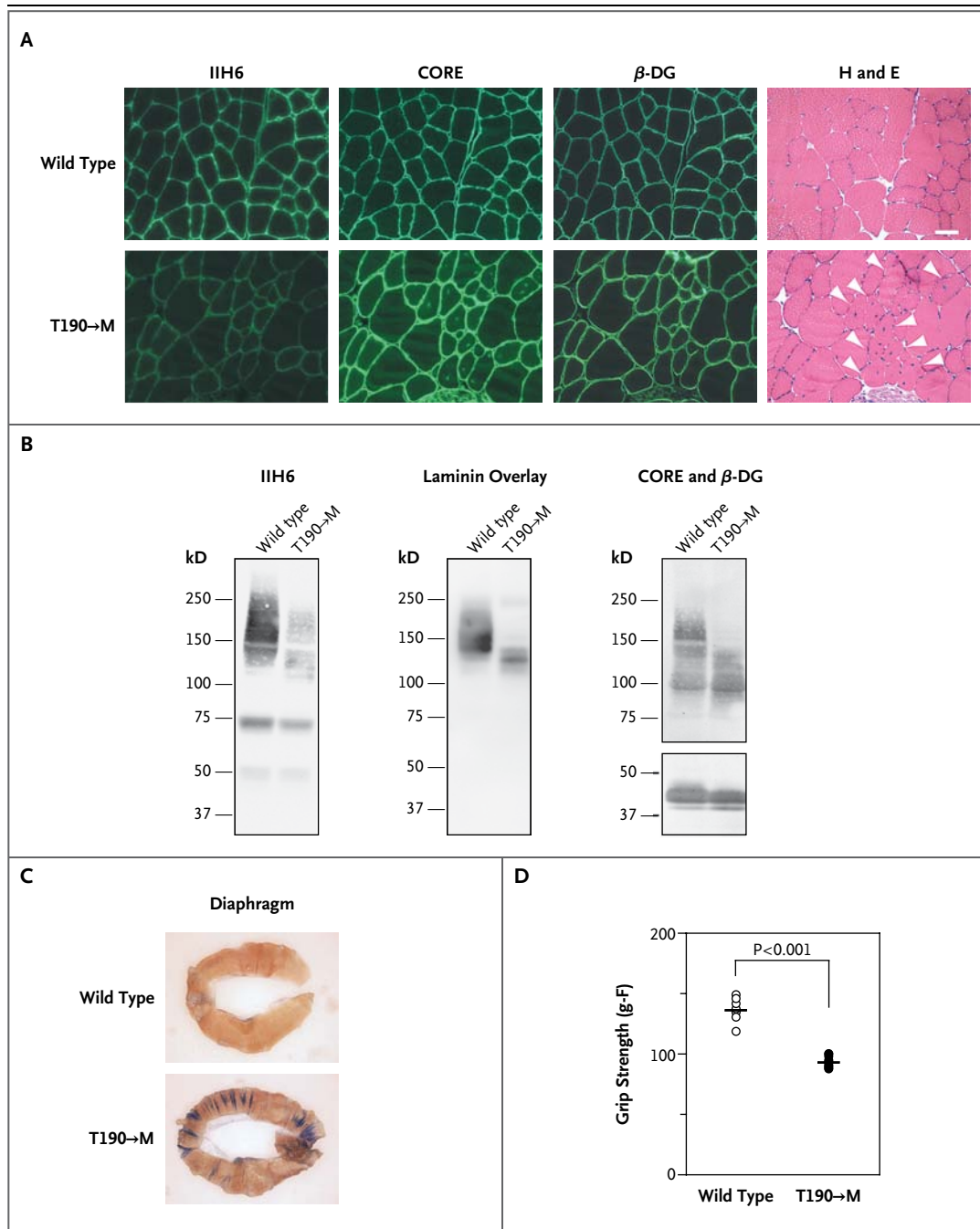
Mutations in *LARGE* have been identified in patients with the Walker–Warburg syndrome or congenital muscular dystrophy type 1C, as well as in mice with myodystrophy (*Large<sup>myd</sup>*).<sup>9,10,22</sup> We recently found that *LARGE* is essential for phosphorylated O-mannosyl glycans to mature into a form capable of binding laminin.<sup>12</sup> We investigated the glycosylation status of T190→M  $\alpha$ -dystroglycan by subjecting the protein to treatment with cold aqueous hydrofluoric acid, which cleaves phosphoester linkages, and to inorganic metal-affinity chromatography, which captures monoester-linked phosphorylated compounds. Hy-

**Figure 2 (facing page). Biochemical and Physiological Skeletal-Muscle Phenotypes of Disease in Gene-Targeted Mice with the Same Dystroglycan Mutation as the Patient.**

Panel A shows immunofluorescence and histologic analyses of T190→M skeletal-muscle (iliopsoas) sections prepared when the animals were 21 weeks of age. Serial sections were stained with antibodies against glycosylated  $\alpha$ -dystroglycan (IIH6), the  $\alpha$ -dystroglycan core (CORE), and  $\beta$ -dystroglycan ( $\beta$ -DG). Histologic abnormalities in the sections were evaluated by means of hematoxylin and eosin (H and E) staining. White arrowheads indicate centrally nucleated fibers (scale bar, 50  $\mu$ m). Panel B shows a representative biochemical analysis of wild-type (WT) and T190→M  $\alpha$ -dystroglycan isolated from wheat-germ agglutinin-enriched homogenates of skeletal muscle. Both Western blotting and laminin-overlay assays were carried out. Functional modification of  $\alpha$ -dystroglycan was impaired by the T190→M mutation in vivo, as shown by the dramatic reduction in IIH6 immunoreactivity and laminin binding in the absence of major differences in CORE and  $\beta$ -DG immunoreactivity. Panel C shows the uptake of Evans blue dye in the diaphragm after exercise in wild-type and T190→M mice at 8 weeks of age. Panel D shows the whole-mouse grip-strength measurements, in gram-force (g-F), for the T190→M mice and their wild-type littermates. The P value was obtained with the use of Student's t-test.

drofluoric acid treatment clearly reduced the molecular weight of T190→M  $\alpha$ -dystroglycan, and the beads on chromatography failed to capture T190→M  $\alpha$ -dystroglycan, although they readily bound  $\alpha$ -dystroglycan in samples from *Large<sup>myd</sup>* animals (Fig. 10 in the Supplementary Appendix). These results suggest that T190→M  $\alpha$ -dystroglycan bears phosphorylated O-mannosyl glycans but that these moieties are not sufficiently mature to confer laminin-receptor function on  $\alpha$ -dystroglycan.

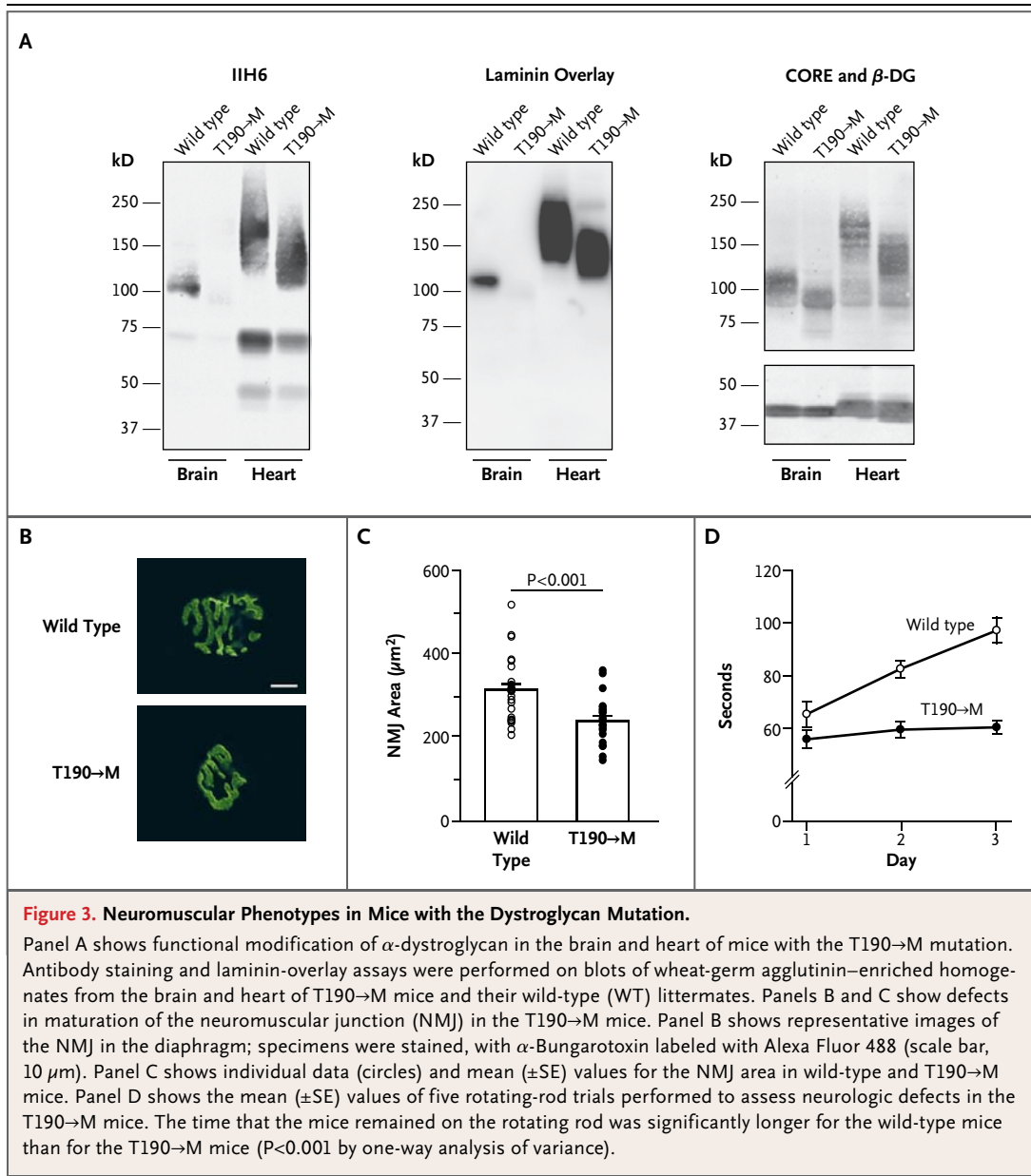
Our findings suggest that the T192→M mutation affects *LARGE*-dependent modification of  $\alpha$ -dystroglycan. A previous study showed that the dystroglycan N-terminal serves as a binding site for *LARGE*, an interaction that is essential for  $\alpha$ -dystroglycan's laminin-binding activity.<sup>15</sup> An in silico model suggested that the side chain of the methionine residue could affect the protein surface structure<sup>23</sup> (Fig. 11A in the Supplementary Appendix); accordingly, we hypothesized that the T192→M mutation abrogates the dystroglycan–*LARGE* interaction owing to a conformational change in the dystroglycan N-terminal. A pull-down assay with Fc-tagged  $\alpha$ -dystroglycan mutants showed that although the wild-type pro-



tein bound to LARGE, variants harboring the T192→M mutation did not (Fig. 11B and 11C in the Supplementary Appendix). These findings support the notion that the T192→M mutation in dystroglycan dramatically impairs the interaction between  $\alpha$ -dystroglycan and LARGE, leading to incomplete post-translational modification of  $\alpha$ -dystroglycan.

## DISCUSSION

Although genes responsible for O-glycosylation-dependent muscular dystrophy (i.e., dystroglycanopathy) have been identified, the molecular mechanisms whereby mutations therein lead to impaired skeletal-muscle and brain function remain elusive — in part because defects in dystro-



glycan itself have not been reported. Here we describe such a case, which represents a new disease class (i.e., primary dystroglycanopathy). The T192→M mutation in this case caused deficiencies in  $\alpha$ -dystroglycan glycosylation and a marked reduction in  $\alpha$ -dystroglycan's ability to bind extracellular-matrix components. Furthermore, our knock-in mouse model harboring the patient's mutation recapitulates the phenotype of secondary dystroglycanopathies in humans, supporting the view that dystroglycan is the main — and probably only — protein that is subject to the

glycosylation abnormalities that cause muscular dystrophy.

Patients with dystroglycanopathy have a broad spectrum of disease phenotypes, with or without brain involvement. Limb-girdle muscular dystrophy with mental retardation was diagnosed in our patient according to the classification system established by Godfrey et al.<sup>13</sup> Biochemical findings from analyses of mouse T190→M show that laminin-binding activity is considerably reduced (Fig. 1 and 2), suggesting that residual glycosylation may account for the relatively mild

muscle phenotype, as compared with the findings in patients with other congenital muscular dystrophies.

Our patient had severe cognitive impairment, yet MRI revealed no gross structural abnormality in the brain.<sup>14</sup> In more severe cases of human dystroglycanopathy, as well as in mice with a brain-specific *Dag1* knockout, structural as well as functional brain abnormalities have been documented.<sup>3-6,9,10,16</sup> Thus, it may be that residual laminin binding by human T192→M dystroglycan is sufficient for the development of the cerebral layer but not for the establishment of normal synaptic physiology. It remains unclear how dystroglycan contributes to synaptic physiology; however, reports that synaptic components possessing laminin globular domains play a fundamental role in establishing and maintaining synaptic function<sup>24,25</sup> suggest that a reduction in the affinity of dystroglycan for synaptic proteins could be responsible for the neurologic phenotypes observed in the patient described here.

Our biochemical analyses show that the T192→M mutation impairs maturation of a specific modification of phosphorylated O-mannosyl glycans on  $\alpha$ -dystroglycan (Fig. 10 in the Supplementary Appendix). In the heart, T190→M  $\alpha$ -dystroglycan maintains substantial laminin-binding activity despite a reduction in molecular weight consistent with that in skeletal muscle and brain (Fig. 2 and 3A), and this remaining activity may contribute to preserved cardiac function (Fig. 8 in the Supplementary Appendix). The tissue variability in levels of  $\alpha$ -dystroglycan's functional glycosylation remains unexplained,

but there are several possible explanations (e.g., tissue-specific protein complexes might increase the affinity between dystroglycan and LARGE, or the enzymatic activity of LARGE might be enhanced in heart tissue). Further investigation will be required to delineate the tissue-specific mechanisms ensuring that phosphorylated O-mannosyl residues of  $\alpha$ -dystroglycan mature into laminin-binding glycans.

In conclusion, we found a pathogenic missense mutation in *DAG1* that selectively impairs further modification of phosphorylated O-mannosyl glycans on  $\alpha$ -dystroglycan, leading to neuromuscular abnormalities. Our findings constitute evidence for the inclusion of *DAG1* in the list of genes whose mutations cause muscular dystrophy and cognitive impairment in humans.

Disclosure forms provided by the authors are available with the full text of this article at NEJM.org.

Supported in part by grants from the Senator Paul D. Wellstone Muscular Dystrophy Cooperative Research Center (1U54NS053672, to Dr. Campbell), the Hacettepe University Research Fund (03.02.101.009, TÜBİTAK Project SBAG-1774, to Dr. Dinçer), the National Institutes of Health (AI45927, to Dr. Oldstone), the National Institute of Diabetes and Digestive and Kidney Diseases (P30 DK 54759, to the University of Iowa Gene Transfer Vector Core), and the Muscular Dystrophy Campaign and Institute of Child Health Biomedical Research Centre (to Dr. Muntoni). Dr. Campbell is an investigator at the Howard Hughes Medical Institute.

We thank Harry Schachter, Michael Anderson, Michael Henry, and Charles Harata for their critical comments; Matthew Goddeeris, Colleen Campbell, Holly Harper, Sally Prouty, Mary Anderson, Keith Garringer, and members of the Campbell laboratory for their scientific contributions; Baoli Yang and Eileen Sweezer (University of Iowa Gene Targeting Core Facility) for generating the T190→M dystroglycan knock-in mice; Lydia Sorokin (Münster University) for the antibody against the laminin  $\alpha 1$  chain (clone no. 317); and the University of Iowa Gene Transfer Vector Core for adenovirus purification.

## REFERENCES

1. Ibraghimov-Beskrovnaya O, Ervasti JM, Leveille CJ, Slaughter CA, Sernett SW, Campbell KP. Primary structure of dystrophin-associated glycoproteins linking dystrophin to the extracellular matrix. *Nature* 1992;355:696-702.
2. Barresi R, Campbell KP. Dystroglycan: from biosynthesis to pathogenesis of human disease. *J Cell Sci* 2006;119:199-207.
3. Michele DE, Barresi R, Kanagawa M, et al. Post-translational disruption of dystroglycan-ligand interactions in congenital muscular dystrophies. *Nature* 2002;418:417-22.
4. Beltrán-Valero de Bernabé D, Currier S, Steinbrecher A, et al. Mutations in the O-mannosyltransferase gene *POMT1* give rise to the severe neuronal migration disorder Walker-Warburg syndrome. *Am J Hum Genet* 2002;71:1033-43.
5. van Rееuwijk J, Janssen M, van den Elzen C, et al. *POMT2* mutations cause  $\alpha$ -dystroglycan hypoglycosylation and Walker-Warburg syndrome. *J Med Genet* 2005;42:907-12.
6. Yoshida A, Kobayashi K, Many H, et al. Muscular dystrophy and neuronal migration disorder caused by mutations in a glycosyltransferase, *POMGnT1*. *Dev Cell* 2001;1:717-24.
7. Kobayashi K, Nakahori Y, Miyake M, et al. An ancient retrotransposal insertion causes Fukuyama-type congenital muscular dystrophy. *Nature* 1998;394:388-92.
8. Brockington M, Blake DJ, Prandini P, et al. Mutations in the fukutin-related protein gene (*FKRP*) cause a form of congenital muscular dystrophy with secondary laminin  $\alpha 2$  deficiency and abnormal glycosylation of  $\alpha$ -dystroglycan. *Am J Hum Genet* 2001;69:1198-209.
9. Longman C, Brockington M, Torelli S, et al. Mutations in the human *LARGE* gene cause MDC1D, a novel form of congenital muscular dystrophy with severe mental retardation and abnormal glycosylation of  $\alpha$ -dystroglycan. *Hum Mol Genet* 2003;12:2853-61.
10. van Rееuwijk J, Grewal PK, Salih MA, et al. Intragenic deletion in the *LARGE* gene causes Walker-Warburg syndrome. *Hum Genet* 2007;121:685-90.
11. Mercuri E, Messina S, Bruno C, et al.

- Congenital muscular dystrophies with defective glycosylation of dystroglycan: a population study. *Neurology* 2009;72:1802-9.
12. Yoshida-Moriguchi T, Yu L, Stalnakier SH, et al. O-mannosyl phosphorylation of alpha-dystroglycan is required for laminin binding. *Science* 2010;327:88-92.
  13. Godfrey C, Clement E, Mein R, et al. Refining genotype phenotype correlations in muscular dystrophies with defective glycosylation of dystroglycan. *Brain* 2007;130:2725-35.
  14. Dinçer P, Balci B, Yuva Y, et al. A novel form of recessive limb girdle muscular dystrophy with mental retardation and abnormal expression of  $\alpha$ -dystroglycan. *Neuromuscul Disord* 2003;13:771-8.
  15. Kanagawa M, Saito F, Kunz S, et al. Molecular recognition by LARGE is essential for expression of functional dystroglycan. *Cell* 2004;117:953-64.
  16. Moore SA, Saito F, Chen J, et al. Deletion of brain dystroglycan recapitulates aspects of congenital muscular dystrophy. *Nature* 2002;418:422-5.
  17. Côté PD, Moukhles H, Lindenbaum M, Carbonetto S. Chimaeric mice deficient in dystroglycans develop muscular dystrophy and have disrupted myoneural synapses. *Nat Genet* 1999;23:338-42.
  18. Nishimune H, Valdez G, Jarad G, et al. Laminins promote postsynaptic maturation by an autocrine mechanism at the neuromuscular junction. *J Cell Biol* 2008;182:1201-15.
  19. Michele DE, Kabaeva Z, Davis SL, Weiss RM, Campbell KP. Dystroglycan matrix receptor function in cardiac myocytes is important for limiting activity-induced myocardial damage. *Circ Res* 2009;105:984-93.
  20. Murakami T, Hayashi YK, Noguchi S, et al. Fukutin gene mutations cause dilated cardiomyopathy with minimal muscle weakness. *Ann Neurol* 2006;60:597-602.
  21. Mercuri E, Brockington M, Straub V, et al. Phenotypic spectrum associated with mutations in the fukutin-related protein gene. *Ann Neurol* 2003;53:537-42.
  22. Grewal PK, Holzfeind PJ, Bittner RE, Hewitt JE. Mutant glycosyltransferase and altered glycosylation of  $\alpha$ -dystroglycan in the myodystrophy mouse. *Nat Genet* 2001;28:151-4.
  23. Bozic D, Sciandra F, Lamba D, Braccaccio A. The structure of the N-terminal region of murine skeletal muscle  $\alpha$ -dystroglycan discloses a modular architecture. *J Biol Chem* 2004;279:44812-6.
  24. Südhof TC. Neuroligins and neuexins link synaptic function to cognitive disease. *Nature* 2008;455:903-11.
  25. Sato S, Omori Y, Katoh K, et al. Pknoxin, a dystroglycan ligand, is essential for photoreceptor ribbon synapse formation. *Nat Neurosci* 2008;11:923-31.

Copyright © 2011 Massachusetts Medical Society.

**NEW NEJM APPLICATION FOR iPhone**

The NEJM Image Challenge app brings a popular online feature to the smartphone. Optimized for viewing on the iPhone and iPod Touch, the Image Challenge app lets you test your diagnostic skills anytime, anywhere. The Image Challenge app randomly selects from 300 challenging clinical photos published in NEJM, with a new image added each week. View an image, choose your answer, get immediate feedback, and see how others answered. The Image Challenge app is available at the iTunes App Store.

## SUPPLEMENTARY METHODS

### Additional clinical information

Clinical data on this patient were reported previously<sup>14</sup>. Briefly, the onset of disease occurred at approximately three years of age, shortly after the patient started to walk. Her initial difficulties were an unsteady gait and difficulty climbing stairs. She has mild calf enlargement and ankle contractures, as well as increased lumbar lordosis. The patient was independently ambulant, but only for short distances (25-30 meters) at 16 years of age. Her intellectual development has been slow: she said her first few words at 7 years of age, and she used only two-word sentences at 16 years of age. At age 16 her IQ was 50, and she was unable to count money and perform independent activities. The creatine kinase concentration at the age of 15 was 4133 U/L. Her cranial MRI was normal.

### Cell culture

The dystroglycan<sup>-/-</sup> myoblast cell line was established as previously described<sup>26</sup>. Briefly, Dystroglycan<sup>flox/flox</sup> mice were crossed with H-2Kb-tsA58 transgenic mice<sup>26,27</sup>, and limb muscles from E18.5 dystroglycan<sup>flox/flox</sup>; H-2Kb-tsA58 embryos were dissociated with 0.2% trypsin and 0.01% DNase. Cells were resuspended in growth medium (DMEM, 1 mM glutamine, 4.5 mg/ml glucose, 10% FBS, 10% horse serum, 0.5% chick embryo extract (Sera Laboratories Inc.), and gentamycin), supplemented with 20 U/ml of recombinant mouse interferon- $\gamma$  (Sigma-Aldrich, I4777, St. Louis, MO) and pre-plated for 20 min at 33°C. Non-adherent cells were transferred to a Matrigel-coated tissue culture dish (BD Falcon, San Jose, CA) and maintained in growth medium at 33°C/10% CO<sub>2</sub>. Dystroglycan<sup>flox/flox</sup> myoblasts that had been screened for their ability to differentiate into myotubes were infected with a pBabe-Cre retroviral vector, and

dystroglycan<sup>-/-</sup> myoblasts were identified by PCR. TSA201, a transformed human kidney cell line stably expressing an SV40 T antigen, was cultured as previously described<sup>15</sup>.

### **Antibodies**

The monoclonal antibody to the glycosylated form of  $\alpha$ -dystroglycan (IIH6), as well as the polyclonal antibody to  $\beta$ -dystroglycan ( $\beta$ DG; ap83), that were used had been characterized previously<sup>3</sup>. The CORE antibody (sheep5, against the  $\alpha$ -dystroglycan core protein) is from sheep antiserum raised against the whole dystrophin-glycoprotein complex and had also been characterized previously<sup>3</sup>. Anti-laminin (L9393), and anti-myc tag (clone 4A6) antibodies were purchased from Sigma-Aldrich (St. Louis, MO), and Millipore (Billerica, MA), respectively. Biotinylated anti-human IgG was obtained from Vector Laboratories (Burlingame, CA). An antibody against the Laminin  $\alpha$ 1 chain (clone 317) was a kind gift from Dr. Lydia Sorokin (Münster University, Münster, Germany).

### **Vector construction**

The T192M-dystroglycan mutation was introduced into expression vectors encoding rabbit dystroglycan, using a conventional PCR method. To generate adenoviral vectors expressing the T192M-dystroglycan mutant, we subcloned a full-length cDNA carrying the T192M mutation into the HindIII and NotI sites of the vector pAd5RSVK-NpA (obtained from the University of Iowa Gene Transfer Vector Core). Adenoviral vectors were generated as described elsewhere<sup>15</sup>. Construction of expression vectors encoding Fc2 (the dystroglycan N-terminus) or Fc5 ( $\alpha$ -dystroglycan) were described elsewhere<sup>15</sup>.

### **Biochemical and ligand-binding analyses**

Glycoprotein enrichment and Western blotting were performed as described previously, with minor modifications<sup>3,15</sup>.

For the cell-surface biotinylation assay, myoblasts infected by adenoviruses expressing WT- or T192M-dystroglycan were washed three times with ice-cold PBS (-) and incubated with PBS (-) containing the membrane impermeable sulfo-NHS-LC-biotin reagent (PIERCE, Rockford, IL) for one hour at 4°C. The cells were then washed twice at room temperature with PBS (-) containing 100 mM glycine, to quench the cross-linker and remove excess biotin. Cells were rinsed in PBS (-) and lysed in Buffer A (150 mM NaCl, 50 mM Tris, pH 7.5) plus 1% Triton X-100 containing a cocktail of protease inhibitors. Cell-surface proteins were immunoprecipitated from the biotin-labeled cells using ImmunoPure Immobilized Streptavidin (PIERCE, Rockford, IL). The samples were then analyzed by Western blotting with the IHH6, CORE, and  $\beta$ DG antibodies.

For the pull-down assay, fusion proteins encoding full-length  $\alpha$ -dystroglycan and the  $\alpha$ -dystroglycan N-terminus bearing the T192M mutation and attached to Fc (Fc5 and Fc2, respectively) were expressed independently in TSA201 cells and purified from the cell lysates using Protein-A affinity beads<sup>15</sup>. The affinity bead-DG-Fc fusion protein complexes were then incubated with lysates from TSA201 cells expressing myc-tagged LARGE<sup>28</sup>. Materials bound to the beads were eluted with Laemmli sample buffer and analyzed by Western blotting. Binding between dystroglycan and LARGE was detected using the Odyssey infrared imaging system (LI-COR Biosciences, Lincoln, NE).

Ligand overlay and laminin solid-phase assays were performed as previously described<sup>3,15,29</sup>.

To analyze laminin clustering, dystroglycan-null myoblast cell-line was infected with adenoviral vectors, at an MOI of 1000, in growth medium. At 24 hours post-infection, cells were seeded onto 8-well glass slides (BD biosciences, San Jose, CA) coated with fibronectin (Sigma-Aldrich, St. Louis, MO). After an additional 24 hours of incubation, the culture medium was replaced with fresh medium containing 7.5 nM mouse EHS Laminin-I (Invitrogen, Carlsbad, CA) and the cells were incubated in this medium for 16 hrs. After fixation (4% paraformaldehyde) and blocking, the cells were

co-stained with the anti-Laminin  $\alpha$ 1 chain (clone No. 317) and CORE antibodies. Confocal microscopy images were analyzed using FV10 ver-1.5 (Olympus, Center Valley, PA). Data show the mean  $\pm$  s.e.m. for three independent experiments.

### **Generation of the T190M-dystroglycan knock-in mice**

Genomic fragments of the mouse *Dag1* gene were isolated from a 129/Sv genomic library<sup>30</sup>. The nucleotide sequence encoding Thr-190 (GTC CTT ACA GTG ATT) was mutated to encode a methionine, and a CviAII restriction site was introduced simultaneously (sequence of the mutant allele: GTC CTC **ATG** GTG ATT; the methionine codon is shown in bold, and the CviAII site is underlined). The Neo cassette flanked by LoxP sites was inserted into a SalI site located between exon 2 and exon 3. A thymidine kinase cassette was attached to the 5' end of the vector for negative selection. The NotI-linearized construct was electroporated into R1 ES cells, and cell clones resistant to positive and negative selection were screened by PCR over the 5' and 3' sides of the insertion. Positive ES clones were microinjected into C57BL/6J blastocysts to generate chimeric mice. PCR-based genotyping of each locus was carried out using the following primers: 5'-homologous recombination: #5742 (5'-CGTCCGCCCTTTCTGTTCTGGTTACTC -3') and #5737 (5'-GCGGGGCTGCTAAAGCGCATGCTCCAGA -3'); 3'- homologous recombination: #5856 (5'-CATCGCCTTCTATCGCCTTCTTGACGAGTT -3') and #5857 (5'-CTCTTCTGAGGCACATCTCCATCACG -3'). To confirm that the T190M mutation was present in the *Dag1* locus, we amplified the mutation-containing DNA fragment (426 bp) using the following primers: #5530 (5'-TGATGGTAACATTTATAACTCACAC-3') and #5531 (5'-GTTGTGAAGTTCTACTTCTGAGAAGCTC-3'). The resultant fragment was digested with CviAII (New England Labs, Ipswich, MA), yielding bands of 327 and 99 bp from the T190M-encoding allele.

### **Analysis of the T190M-dystroglycan knock-in mice**

Immunofluorescence analysis and hematoxylin-eosin staining were carried out as described previously<sup>3</sup>. For the fore-limb grip-strength test, T190M (n=10) and littermate control (WT; n=9) mice at 11-20 weeks of age were examined using a grip-strength meter (Columbus Instruments, Columbus, OH, model #1027). This test was repeated five consecutive times within the same session, and the means of all trials were recorded. For analysis of NMJs with Alexa488-labelled  $\alpha$ -bungarotoxin, diaphragm sections (30-40  $\mu$ m) or whole diaphragm samples were prepared from adult T190M knock-in mice or their littermate controls. Those samples were fixed with 4% paraformaldehyde in PBS (sections: for 20 min; whole diaphragm: for three hours), and permeabilized with 0.5% Triton X-100 in PBS for 10 min on ice. After blocking with 3% BSA in PBS, the sections were incubated with Alexa488-labeled  $\alpha$ -bungarotoxin (Invitrogen, Carlsbad, CA) overnight at 4°C. Images were taken using a confocal microscope (FV10 ver-1.5, Olympus, Center Valley, PA), and analyzed using the Image Pro plus program (Media Cybernetics, Bethesda, MD). For Evan's blue dye (EBD) uptake assay, adult T190M knock-in mice and littermate controls were injected with EBD one day before exercise. Those mice were subjected to downhill running on a treadmill with a built-in shock grid at a 15 degree declination. After a warm-up running (3 m/min, 5 minutes), the initial running speed of 10 m/min was increased every 5 minutes by 5 m/min until the maximal speed (25 m/min) was reached. Exhaustion was defined as the point at which the animal would not resume running. Tissues were harvested at one day after the exercise. In evaluating cardiac muscle pathology, we used skeletal and cardiac muscle-specific (*MCK-cre*) dystroglycan-deficient mice<sup>27</sup> as a control. HFaq treatment and an IMAC bead binding assay were performed as described previously<sup>12</sup>. Rotarod performance was tested in T190M knock-in mice and littermates, 10 to 15 weeks of age, using the ROTOR-ROD system (San Diego Instruments, San Diego, CA). The mice were placed on top of the beam, and the rotarod accelerated gradually, without jerks, from 0 to 35 rpm

over a two-minute trial. Latencies for the mice to fall from the rod were recorded automatically. Each mouse was subjected to 5 trials at 15-min intertrial intervals, on each of three consecutive days.

### **Molecular modeling**

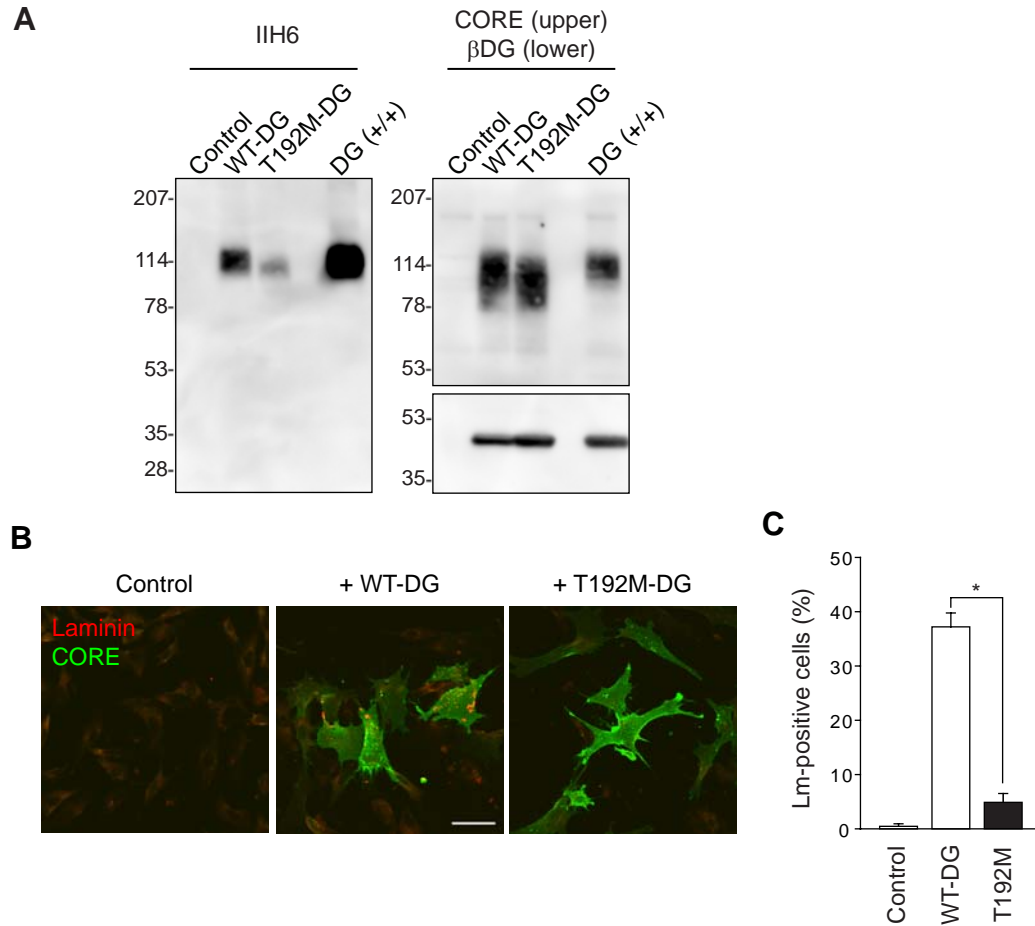
The N-terminal portion of the T192M mutant of  $\alpha$ -dystroglycan was modeled using the SWISS-MODEL program for the analysis, and the crystal structure of the WT mouse orthologue as a template (Ref. 23, PDB accession No. 1u2c). The figure was prepared using the program PyMOL v-0.99 (DeLano, W.L. The PyMOL Molecular Graphics System (2002) DeLano Scientific, San Carlos, CA, <http://www.pymol.org>).

### **Author contributions**

Y.H., P.D. and K.P.C. designed the study. B.B., H.G., B.T., F.M., H.T. and P.D. diagnosed patients, collected blood from the patient, and analyzed genetic data. S.J.B. provided the dystroglycan-null myoblast cell line from our skeletal muscle-specific conditional knockout mice. Y.H. and M.K. performed biochemical studies, with the assistance of T.Y.-M., T.W., S.K. and M.B.A.O. D.B., T.Y.-M., T.W., J.S.S., S.K., M.B.A.O. and F.M. provided critical discussion on the research. Y.H. and R.W.C. performed the mouse studies. Y.H. and A.A. performed the structural modeling studies. K.P.C supervised and mentored all work. Y.H. and K.P.C. wrote the initial manuscript, and all authors contributed to the final version of the manuscript.

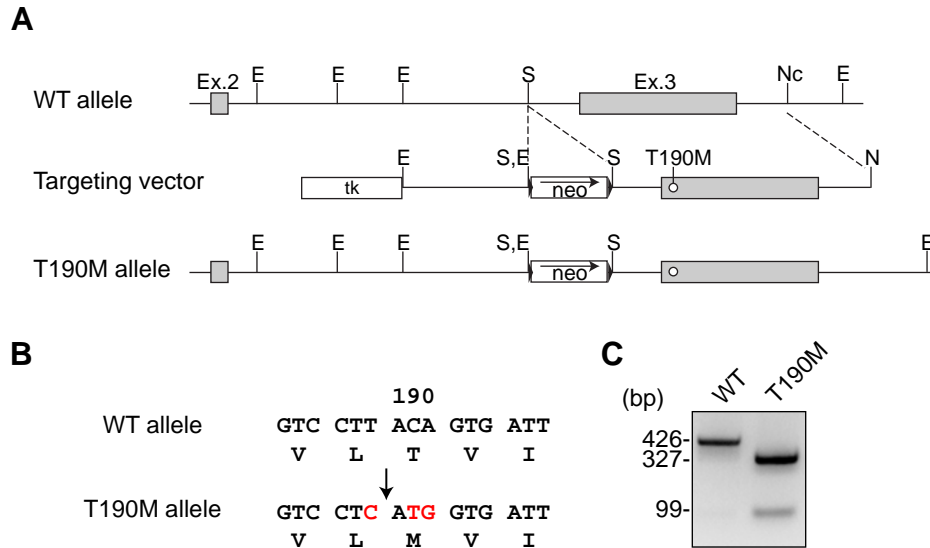
## SUPPLEMENTARY REFERENCES

26. Herbst R, Burden SJ. The juxtamembrane region of MuSK has a critical role in agrin-mediated signaling. *Embo J* 2000;19:67-77.
27. Cohn RD, Henry MD, Michele DE, et al. Disruption of *Dag1* in differentiated skeletal muscle reveals a role for dystroglycan in muscle regeneration. *Cell* 2002;110:639-48.
28. Rojek JM, Campbell KP, Oldstone MB, Kunz S. Old World arenavirus infection interferes with the expression of functional alpha-dystroglycan in the host cell. *Mol Biol Cell* 2007;18:4493-507.
29. Sugita S, Saito F, Tang J, Satz J, Campbell K, Sudhof TC. A stoichiometric complex of neuexins and dystroglycan in brain. *J Cell Biol* 2001;154:435-45.
30. Williamson RA, Henry MD, Daniels KJ, et al. Dystroglycan is essential for early embryonic development: disruption of Reichert's membrane in *Dag1*-null mice. *Hum Mol Genet* 1997;6:831-41.



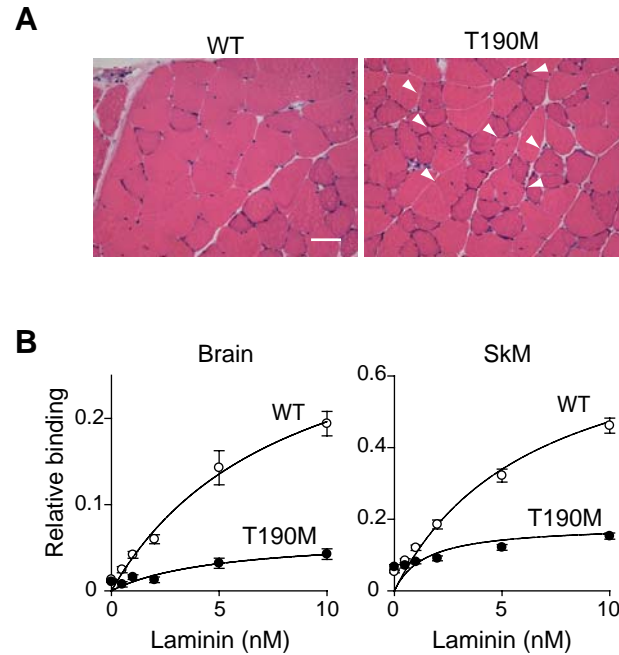
**Supplementary Figure 1 | Biochemical analyses of the WT- and T192M-dystroglycan proteins in dystroglycan-null myoblast cells.**

Panel A shows cell-surface expression of the WT- and T192M-dystroglycan proteins in dystroglycan-null myoblast cells. WT- and T192M-dystroglycan-expressing cells were incubated with EZ-link Sulfo-NHS-LC-biotin. After membrane solubilization, biotinylated proteins were enriched using streptavidin-immobilized beads and subjected to Western blotting with the IIH6, CORE, and  $\beta$ DG antibodies. Panel B shows organization of laminin on the cell surface, in WT- and T192M-dystroglycan-expressing myoblast cells. Laminin clustering was observed only on cells expressing adenovirus-encoded WT-DG. The cells were co-stained with anti-laminin (clone #317) and CORE antibodies. White bar: 50  $\mu$ m. Panel C shows statistical analysis of laminin clustering activity on WT- (open column) and T192M- (filled column) dystroglycan. Asterisk,  $P < 0.001$  (Student's *t*-test).



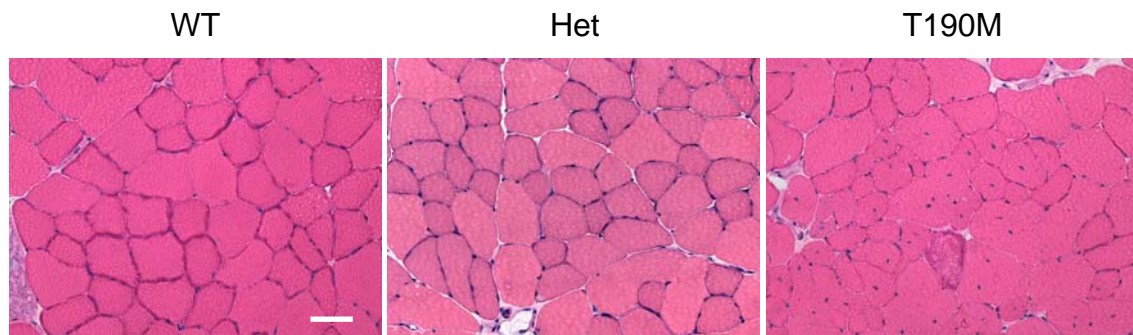
### Supplementary Figure 2 | Generation of a mouse model harboring the T190M mutation.

Panel A shows a schematic representation of the WT *Dag1* allele, the targeting vector, and the homologously recombined allele. The open circle in exon 3 indicates T190M, which corresponds to the human T192M mutation. The thymidine kinase and Neo cassettes are illustrated as boxed tk and Neo, respectively. Filled arrowheads flanking the Neo cassette indicate loxP sites. Selected restriction enzyme cleavage sites are indicated above the gene (E: EcoRI; N: NotI; Nc: NciI; and S: SalI). Panel B shows engineered sequence abnormalities in the T190M knock-in mice, with nucleotide sequence shown at top and amino acid sequence shown at bottom. The knock-in sequence includes a recognition site for the restriction enzyme CviAII (marked by arrow). Panel C shows representative PCR genotyping analysis of the T190M-homozygous (T190M) mice. PCR products containing the T190M mutation are cleaved by CviAII.



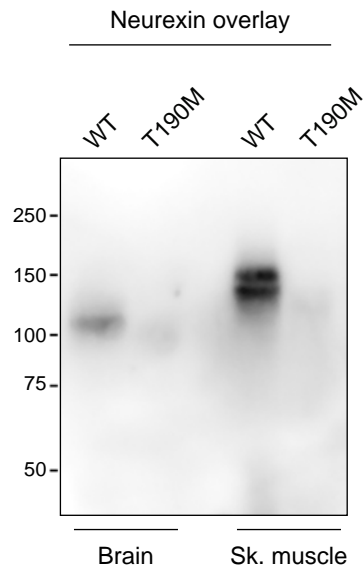
**Supplementary Figure 3 | Further histological and biochemical analyses of a mouse model harboring the T190M mutation.**

Panel A shows H&E-stained sections of gastrocnemius muscle, revealing the presence of centrally located nuclei in this muscle in the T190M mouse at 21 weeks of age. White arrowheads denote pathologic fibers. White bar: 50  $\mu$ m. Panel B summarizes the results of solid-phase laminin-binding assays with WGA homogenates of brain (left) and skeletal muscle (right) from T190M mice and their littermate controls.



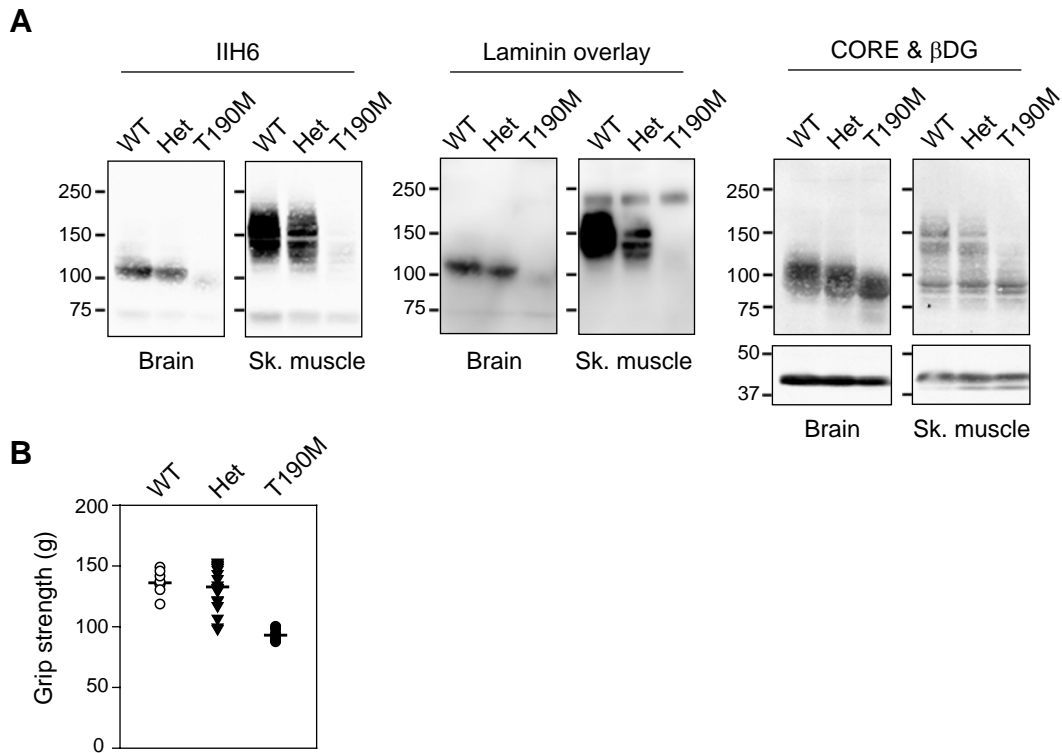
**Supplementary Figure 4 | Histological analysis of one-year-old T190M mice.**

H&E staining of wild-type (WT), heterozygous (Het), and T190M iliopsoas muscle taken from one-year-old mice. Myofibers with centrally localized nuclei were only observed in the homozygous mouse. Scale bar: 50  $\mu\text{m}$ .



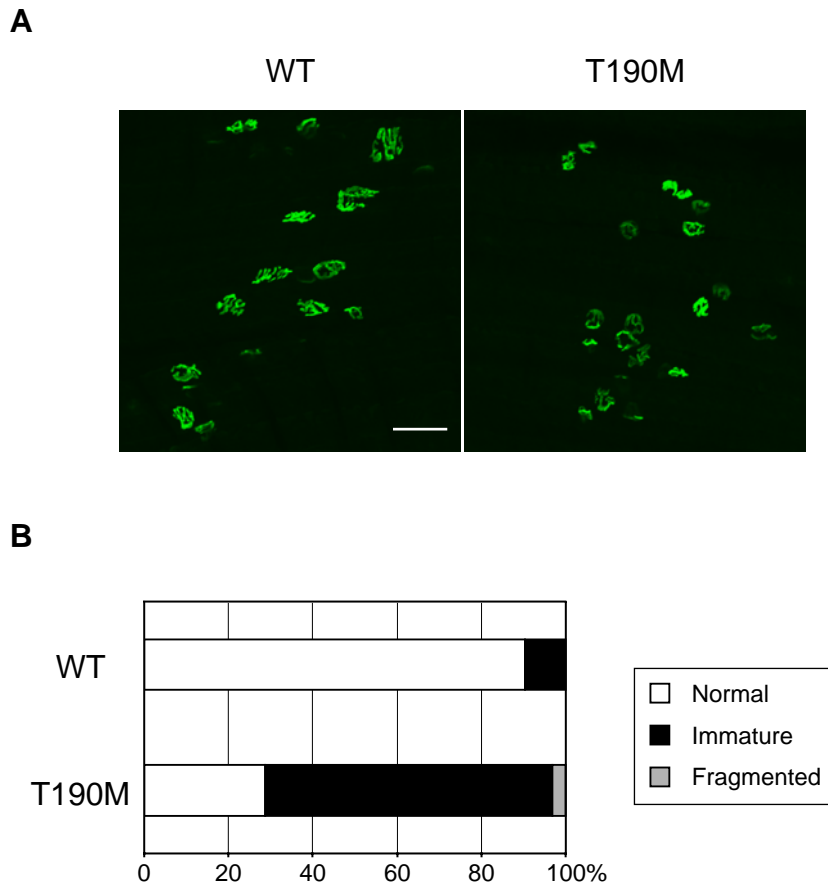
**Supplementary Figure 5 | Neurexin overlay assay with WT- and T190M-dystroglycan**

Representative image of neurexin overlay assay with WT- and T190M-dystroglycan. The membrane of WGA-enriched fractions prepared from WT and T190M mice were subject to the ligand overlay assay, using neurexin-immunoglobulin fusion protein<sup>3,29</sup>. Neurexin binding activity was significantly reduced on T190M-dystroglycan.



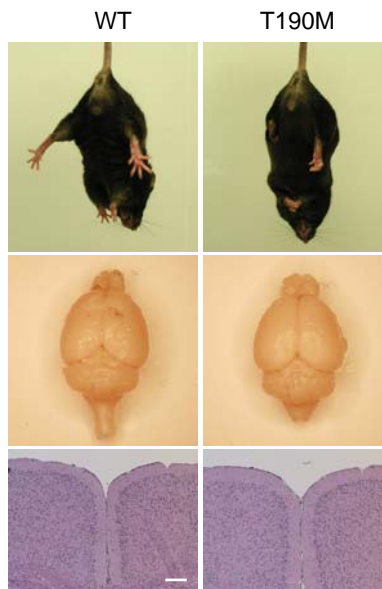
### Supplementary Figure 6 | Phenotypic analysis of T190M heterozygous mice

Panel A shows representative images of Western blot analysis of WT, Het, and T190M mice. Expression and glycosylation of dystroglycan were evaluated using the I1H6 antibody (left), Laminin overlay (middle), and CORE &  $\beta$ DG antibodies (right). Panel B displays results from the grip strength test among WT, Het, and T190M mice. Reduction in grip strength was observed in T190M mice compared with WT and Het mice ( $P < 0.001$ , One-way ANOVA test), but there was no statistical difference between WT and Het mice.



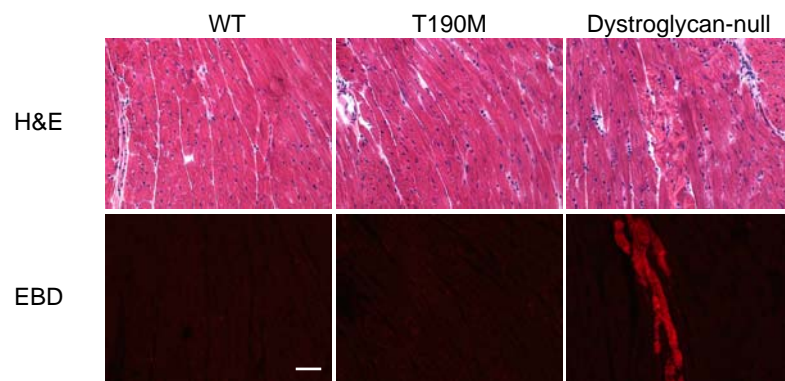
**Supplementary Figure 7 | Morphological analysis of NMJs in WT and T190M diaphragm.**

Panel A shows representative images of NMJs in WT and T190M muscle samples stained with Alexa488-labeled  $\alpha$ -bungarotoxin. Scale bar: 50  $\mu$ m. Note that NMJs in T190M diaphragms tend to be smaller and structurally less complex than those in WT diaphragms. Panel B shows evaluation of NMJ morphology in WT and T190M homozygous mice at the ages of 9-21 weeks old (Diaphragm, n = 218 for WT and n = 366 for T190M homozygous mice).



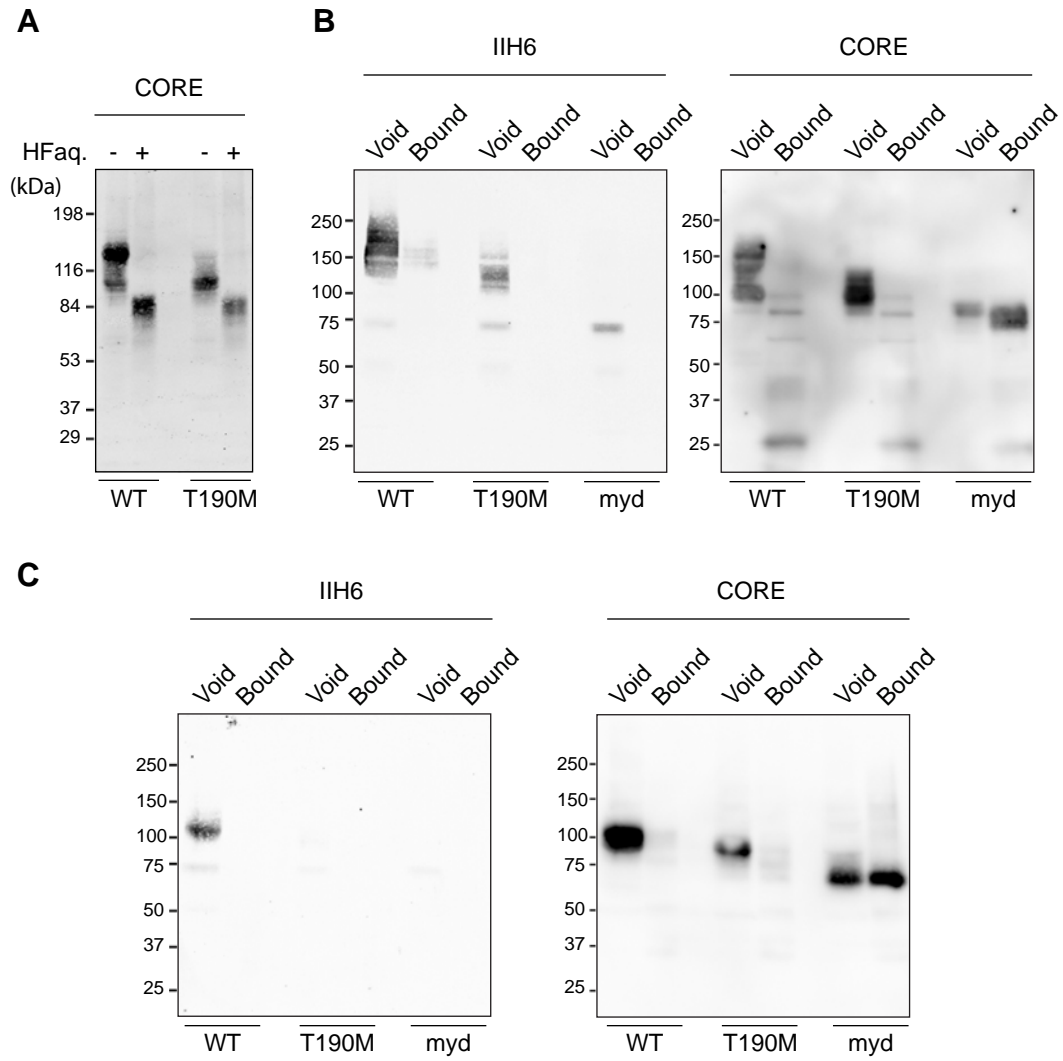
**Supplementary Figure 8 | The T190M mouse model displays neurological phenotypes.**

Top panels show representative WT (left) and T190M (right) mice suspended by the tail. Only mutant mice displayed a clasping phenotype (T190M: 13 out of 19 mice). Middle panels show gross structures of the control and T190M mutant brains. No structural abnormality was evident in the mutant mice. Bottom panels show histological sections of cerebral cortices of WT and T190M mice. H&E staining of the brain sections reveals that neuronal migration in the T190M brain was normal. White bar: 200  $\mu\text{m}$ .



**Supplementary Figure 9 | The T190M mutation does not affect cardiac muscle pathology in response to exercise stress in mouse.**

Upper panels show H&E staining of cardiac sections from WT and T190M mice. Lower panels show Evans blue dye uptake (EBD, in Red) in the heart. Dystroglycan-null hearts were analyzed as negative controls<sup>27</sup>. EBD uptake was observed only in the dystroglycan-null hearts, suggesting that a deficiency in dystroglycan function causes susceptibility to exercise-induced cardiac membrane damage. White bar: 50  $\mu$ m.

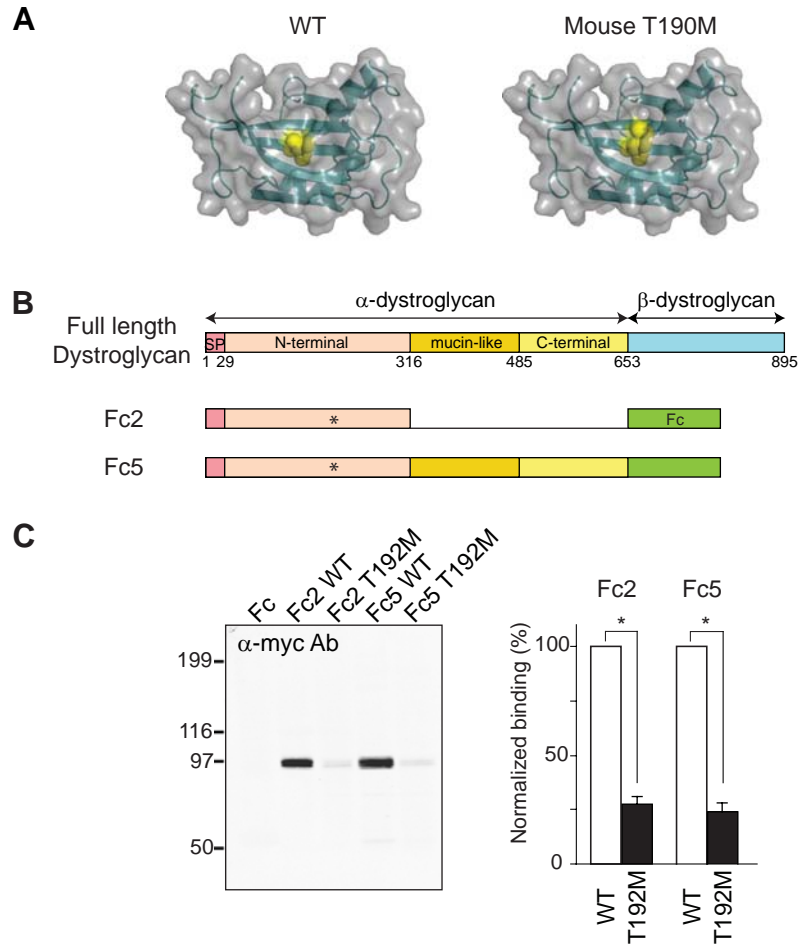


**Supplementary Figure 10 | The T190M mutation impairs maturation of dystroglycan's post-phosphoryl glycans.**

Panel A shows the consequences of chemical dephosphorylation of  $\alpha$ -dystroglycan by treatment with aqueous hydrofluoric acid (HFAQ). WGA-enriched protein fractions of WT and T190M skeletal muscle were subject to HFAQ treatment, which specifically cleaves phosphoester linkages.  $\alpha$ -dystroglycan was detected using the CORE antibody.

The observed reduction in the molecular weight of T190M  $\alpha$ -dystroglycan following HFAQ treatment indicates that further modification occurs on the  $\alpha$ -dystroglycan phosphate residues in the muscle of these animals. Panels B and C show binding of  $\alpha$ -dystroglycan to Immobilized Metal Affinity Chromatography (IMAC) beads.

Glycoproteins from WT, T190M, and *Large<sup>myd</sup>* (myd) muscle (Panel B) and brain (Panel C) samples were applied to IMAC beads. Bound and void fractions were analyzed by Western blotting with the I1H6 and CORE antibodies. Neither WT nor T190M  $\alpha$ -dystroglycan bound to the beads, whereas myd  $\alpha$ -dystroglycan was captured by the beads.



**Supplementary Figure 11 | The T192M mutation disrupts the molecular interaction between dystroglycan and LARGE.**

Panel A shows models of the RNA binding protein-like domain of the mouse dystroglycan N-terminus, based on the crystal structure of the WT dystroglycan N-terminus<sup>23</sup>. The model of the WT protein is shown on the left, and an *in silico* model of the mouse T190M mutant is shown on the right. Thr-190 and the mutated residues are indicated in yellow. The domain is displayed in surface representation, with ribbon diagrams superimposed (cyan). The crystal structure of the WT mouse dystroglycan N-terminus shows that Thr-190 is located in the middle of a cleft, with its side chain exposed<sup>23</sup>. In the *in-silico* model of the mouse T190M mutant protein, the overall fold is conserved but the bulky methionine side chain protrudes into the cleft, partially occluding it. Panel B shows a schematic representation of the  $\alpha$ -dystroglycan:Fc fusion proteins. Fc5 ( $\alpha$ -dystroglycan-Fc) and Fc2 (the dystroglycan N-terminus-Fc) were used for pull-down assays with LARGE. The position of residue Thr-192 is indicated by an asterisk. Panel C demonstrates that the dystroglycan N-terminus interacts molecularly with LARGE. (Left) A representative result from the pull-down assay, carried out with myc-tagged LARGE and an anti-myc antibody. (Right) Quantification of LARGE-binding activity by WT (open columns) and mutant (T192M, filled columns) dystroglycan-Fc proteins. Asterisk,  $P < 0.001$  (Student's *t*-test).